Results in Geophysical Sciences 11 (2022) 100044

Contents lists available at ScienceDirect

Results in Geophysical Sciences

journal homepage: www.sciencedirect.com/journal/results-in-geophysical-sciences

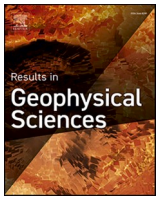

Pressure and temperature dependence of the relaxation of the electrical double layer in hydrated magnesite rock (leukolite)

Anthony N. Papathanassiou [a,*], Elias Sakellis [a,b]

[a] National and Kapodistrian University of Athens, Physics Department, Section of Condensed Matter Physics, Panepistimioupolis, GR 15784 Zografos, Athens, Greece
[b] National Center of Natural Sciences Demokritos, Institute of Nanomaterials and Nanotechology, Aghia Paraskevi, Athens, Greece

ARTICLE INFO

Keywords:
Rocks
Electrical double layer
Relaxation
Pressure

ABSTRACT

The introduction of water into the pore space of naturally occurring magnesite (leukolite) induces an intense relaxation mechanism, which is related to the electric double layer (EDL) formed on opposing sides of the solid – mater interface. The relaxation of the EDL is studied by using Broadband Dielectric Spectroscopy at different conditions of combined temperature and hydrostatic pressure. The temperature evolution of the characteristic relaxation frequency, reveals two successive temperature regions: in the low temperature one, protonic conductivity over the network of water molecules in on the solid surface, couples to the ionic transport of charged defects occurring in the solid. At higher temperatures, near – zero activation energies are found: the phenomenon is discussed theoretically and attributed to decoupling and an exchange of protons with lattice site magnesium cations, the formation of a proton enriched sub-surface layer of magnesite and subsequent release of cations to the liquid. The values of the activation volume and their independence on temperature, support the aforementioned interpretation.

1. Introduction

Porous materials provide large surface area to interact with fluids. Water wetting the interior of the pore space of rocks changes their overall electric and dielectric properties. The effective dielectric constant is considerable enhanced even by the presence of traces of water molecules or humidity and its value exceeds by far the weighted average of those of water and dry rock (Endres and Knight, 1991; Nettelblad, 1996; Papathanassiou, 2000). Effective mean field theories proposed by Maxwell, improved by Wagner (1924) and revisited by Hanai (1986) assume that the individual phases do not interact with each other, e.g., by charge exchange or in-homogeneous distribution of the charge density. In these theories, which are quite good to interpret the experimental results, the effective frequency dependent dielectric permittivity and dc conductivity obey a mixing rule of the ones of the end components and their geometrical characteristics. Furthermore, more refined models, include the solid-liquid interaction, in terms of the formation of an electrochemical double layer. It occurs whenever materials of different conductivity form a junction (such as, a metal in contact with a liquid, a p-n junction of semiconductors with different doping level, rock grains wetted by water or oil). The distribution of electric charge on both sides of the interface of a solid – water varies upon the distance from each interface. Successive layers of water molecules cover the solid surface: the water molecules attaching the solid surface constitute the Stern layer; those on upper layers are more mobile and form the so-called diffusion region. Moreover, charge exchange can occur among the solid and liquid phases is likely to occur (Revil and Glover, 1997).

Alkaline earth carbonate salts, such as calcite ($CaCO_3$), magnesite ($MgCO_3$) and dolomite ($(CaMg(CO_3)_2$), are rock forming materials of the earth's solid crust. For example, calcite forms limestone and magnesite can be found as leukolite. Water wetting the surface of an alkaline earth carbonate salt is organized to form a single – molecule layer on the solid (usually termed as the Stern layer)whereas the bound polar molecules have reduced degrees of rotational and translation motion in relation to those of overlying layers (usually termed as diffuse layer of "bulk" water). Water molecules in the Stern layer constitute a network of significant protonic surface conductivity, which exceeds the molecular drift or diffusion. The synergy of the aforementioned parameters determines the dynamics of the water – matrix systems perturbed by external time – varying electric fields. The response and relaxation is described in terms of a (dielectric relaxation time τ, which is a phenomenological time – constant or, alternatively, equals or proportional to the inverse of the

* Corresponding author.
E-mail address: antpapa@phys.uoa.gr (A.N. Papathanassiou).

https://doi.org/10.1016/j.ringps.2022.100044
Received 25 March 2022; Received in revised form 13 June 2022; Accepted 10 August 2022
Available online 22 August 2022

mean microscopic transition rate of relaxing species.

More or less, water is wetting their porosity, electrical double layers (EDLs) are formed. Spectroscopy (such as Nuclear Magnetic Resonance (NMR) (Korb, 2018) and Broadband Dielectric Spectroscopy (BDS)) can correlate frequency resonances with the dynamics of EDL in confinement conditions (Saltas et al., 2008; Saltas et al., 2013; Saltas and Gidarakos, 2013; Saltas et al., 2014). The knowledge gained is valuable in many diverging fields of science and technology: materials science

Among different naturally occurring single crystals and rocks, either dry or hydrated at various levels, studied by time domain and Broadband Dielectric Spectroscopy (BDS), an unconventional pressure dependence of the dielectric relaxation was traced in hydrated leukolite (Papathanassiou et al., 2010), limestone (Sakellis et al., 2014) and granodiorite (Papathanassiou et al., 2011) while in most solids dielectric relaxation is retarded on increasing pressure (i.e., the relaxation activation volume is positive), herein, relaxation was boosted on compression and negative activation volume were obtained (Papathanassiou et al., 2010). In the present work, we investigate the EDL relaxation of wetted porous magnesite (leukolite) at elevated pressure and temperature. Activation energy and activation volume as a function of temperature are expected to shed light on the coupling between charge transports along either sides of the Stern layer, i.e., the correlated motion of charges in the solid with the protonic transport along the water network wetting the solid surface. Decoupling is subsequently tuned via temperature and pressure combination. The present work contributes in the field of basic research on the EDL relaxation at P – T states, which is missing from the literature and simulates the conditions occurring in depth of the earth's solid crust. The latter is useful for profiling the response of carbonate rocks hosting water or oil (Chelidze et al., 1999) and for the understanding the origin of seismic electric signals (SES) (Varotsos and Alexopoulos, 1984) and related phenomena (Tzanis and Vallianatos, 2001; Vallianatos et al., 2004; Vallianatos and Triantis, 2008).

2. Theoretical background

The interaction between the surface of a porous solid and water can dominate significantly the overall electrical properties of wetted rocks, due to the development of interfacial layers between the solid and the liquid phases. The structure of these inter-layers and their response to applied electric fields depend on the coupling between surface and volume processes, the EDL at the solid – liquid interface, as well as, the topology and physic-chemical characteristics of the solid and the liquid, respectively Transition rate theory describes equilibrium or relaxation phenomena, The thermodynamics dielectric relaxation is measuring the relaxation times at different temperatures and estimating the activation energy. The measurement of the relaxation time at various pressures yields the activation volume. The temperature dependence of both thermodynamic activation The polarization of adsorbed water stems from the reorientation of water molecules and the proton conductivity along hydroxyl in an organized molecular network.

The surface polarization of a thin film of conducting liquid, with surface conductivity σ_s and surface diffusivity D_s, on the surface of an insulating sphere of radius α, relative dielectric permittivity ε_2 (ε_o is the permittivity of free space),embedded into a matrix of complex permittivity ε^*, is achieved through surface diffusion of electric charges along the interface. The relaxation time is given by Dukhin et al. (1969):

$$\tau = \frac{\alpha^2}{2\left(D_s + \frac{4\pi\alpha}{\varepsilon_o(2\varepsilon_1+\varepsilon_2)}\sigma_s\right)} \tag{1}$$

The surface diffusivity D_s is commonly smaller than the bulk one, because the counter ions inside the Stern layer are more closely bounded around the surface of the solid.

The validity of the Nernst-Einstein to surface processes has been verified for a significant amount of experimental data on porous media wetted by aqueous solutions (Revil, 1999) concluded on a diffusivity – conductivity coupling, in agreement with the pioneering work (Gast and East, 1964), who found an agreement between cation mobility measured by diffusion and electrical conduction:

$$\tau = \frac{\alpha^2}{2D_s\left(1 + \frac{4\pi\alpha}{\varepsilon_o(2\varepsilon_1+\varepsilon_2)}\frac{ce^2}{kT}\right)} \tag{2}$$

where c, depending on the nature of electrical conduction, is proportional to the number density of charge entities involved into the relaxation. Within the frame of the transition rate theory, the relaxation time is participating to the reciprocal microscopic transition frequency or relaxation frequency f_0. Here, we define:$f_0 \equiv 1/\tau$.

For simplicity, we symbolize:

$$x \equiv \frac{4\pi\alpha e^2}{\varepsilon_o(2\varepsilon_1+\varepsilon_2)}c \tag{3}$$

Eq. (2) is re-written as follows:

$$-lnf_o = -lnD_s - ln(1+x) - ln2 + 2ln\alpha \tag{4}$$

In complex impedance measurements, the relaxing species are making optimum use of the energy of the applied field at a resonant frequency f_o. The temperature evolution of the relaxation rate at constant pressure, provides the *apparent* activation energy for relaxation:

(5)

On the other hand, experiments at constant temperature and different pressure yield the *apparent* activation volume:

$$v^{app} \equiv -\left(\frac{\partial nf_o}{\partial P}\right)_P \tag{6}$$

The latter identity is valid under the constrain that the phonon frequencies and, subsequently, the attempt frequency of transferring species have a negligible dependence on pressure, or, the product, where γ and κ_T denote the Gruneisen parameter and the isotherm compressibility, respectively, is much smaller than$\left(\frac{\partial}{\partial P}lnf_o\right)_P$ (for magnesite, $\gamma\kappa_T = 0.0221GPa^{-1}$ (Papathanassiou et al., 2010), which is three orders of magnitude smaller than the measured$v\left(\frac{\partial lnf_o}{\partial P}\right)_P$ values reported below).

3. Experimental methodology

An automated Novocontrol High Pressure Dielectric Spectroscopy apparatus was employed to study dielectric relaxation at iso-static conditions of temperature and hydrostatic pressure, A frequency response analyzer (FRA) Solartron 1260 in series with a Novocontrol Broadband Dielectric Converter were used to perform complex impedance experiments from 10 mHz to 1 MHz. τ is a true, dielectric relaxation time, which is proportional to the relaxation frequency f_o. The proportionality factor is sensitive to the assumptions made in the transition rate theory, such as the dimensionality of the material, its symmetry and the isotropic along different directions in space. As explained above, the value of the proportionality factor does not influence the temperature and pressure derivatives of τ, and can be regarded equal to unity.

A FRA senses relaxation resonance as a maximum in the loss tangent function $tan\ \delta(f) \equiv Im(\varepsilon^*)/Re(\varepsilon^*)$, where Im($\varepsilon^*$) and Re($\varepsilon^*$) are the imaginary and the real part of the (relative) complex permittivity ε^*(f). We stress that an FRA measures directly the phase shift between the output signal in relation to the int harmonic one applied to a test specimen. The peak maximum frequency $f_{max,tan\delta}$ is correlated with the dielectric relaxation rate f_o, according to:$f_{max,tan\delta} = \sqrt{\varepsilon_{stat}/\varepsilon_\infty}f_o$, where ε_{stat} and ε_∞ denote the static and high frequency (relative) permittivity, respectively. These values can be estimated by extrapolation of the available complex permittivity data to the low and high frequency limit, respectively. The temperature and pressure derivatives of the dielectric relaxation rate $f_o \equiv 1/\tau$, is determined from the partial derivatives of

$f_{max,\ tan\delta}$, ε_{stat} and ε_∞ (which are obtained from a complex impedance spectra, is given –within the transition rate theory - by Papathanassiou et al. (2010):

$$\left(\frac{\partial lnf_o}{\partial\left(\frac{1}{kT}\right)}\right)_P = \left(\frac{\partial lnf_{max,tan\delta}}{\partial\left(\frac{1}{kT}\right)}\right)_P - \frac{1}{2}\left(\frac{\partial(\varepsilon_{stat}/\varepsilon_\infty)}{\partial\left(\frac{1}{kT}\right)}\right)_P \quad (7)$$

$$\left(\frac{\partial lnf_o}{\partial P}\right)_T = \left(\frac{\partial lnf_{max,tan\delta}}{\partial P}\right)_T - \frac{1}{2}\left(\frac{\partial(\varepsilon_{stat}/\varepsilon_\infty)}{\partial P}\right)_T \quad (8)$$

4. Materials and methods

Leukolite is one the purest magnesite rock, collected from the large deposits in the island of Euboea, Greece.. Clear snow-like white specimens were inspected with crossed Nicolet transmission optical microscopy through thin sections of the mineral and a porosity of 0.05 was determined. The analysis performed by the Institute of Geological and Mining Research (IGME, Greece) gave the following results: 47.90 wt % MgO, 2.80 wt % Si, 0.02 wt % Al, 0.13 wt % Fe, 0.41 wt % Ca, 0.02 wt % Mn, 0.02 wt % Sr, 0.01 wt % K, 0.04 wt % Na 23 wt % (Papathanassiou, 1999).

Disc shape samples were prepared, with typical, diameter 20 mm and thickness 1-1.5 mm. The removal of any trace of humidity from its porosity was achieved by placing the sample inside a vacuum cryostat: an Alcatel turbo-molecular pump dictated dynamic pressure of 10^{-4} Pa (i.e., 10^{-9} bar) at isothermal conditions ranging from room temperature to 345 K, overnight. Hydration could be achieved by immersing the specimen in doubly distilled and doubly de-ionized water at 343 K for 72 h; air bumbles could be observed on the sample surfaces, due to the out-gassing of its porosity. Subsequently, the system is left to cool down to room temperature (Papathanassiou et al., 2010). An alternative method for hydration was to place the beaker hosting the specimen immersed in water, into a jar whereas dynamic vacuum was dictated to out-gas the rock's porosity. Afterwards, air was left to flow into the jar and, hence, water was subjected to fill the vacant pore space. By weighting the sample prior and after the hydration, we found that the rock is filled with water at a ratio of 1.1-1.4 wt % .

Metal electrodes were silver - pasted on both parallel surfaces of the disk shaped specimen. Subsequently, an ultra thin insulating layer of epoxy covered the specimen to prevent contamination from the pressure transmitting fluid of the High Pressure vessel (Papathanassiou et al., 2000, 2007) and jacket the entire hydrated rock specimen.

5. Results

5.1. Temperature dependence of the EDL relaxation

The tangent loss angle spectra of hydrated leukolite are characterized by an intense peak overlapping with a dc conductivity baseline, as can be seen in Fig. 1. The peak maximum $f_{mx,tan\delta}$ is a function of pressure and temperature, hence, a suitable pressure – temperature combination permits a clear and direct observation of the maximum, of the loss peak. In Fig. 1, *tanδ(f)* isotherms collected at 270 MPa are depicted, together with a reference measurement on a *dry* sample, ensuring that the observed peak is related to wetting.

In Fig. 2, $lnf_{max,tan\delta}$ is plotted against $1/kT$. From room temperature to about 345 K (low temperature region), $lnf_{max,tan\delta}$ shifts gradually toward high frequency, while, above 345K (high temperature region), it is remarkably weakly affected. A straight line fitted to the low temperature data points. Its slope and typical values for ionic crystals for the terms $\left(\frac{\partial(\varepsilon_{stat}/\varepsilon_\infty)}{\partial T}\right)_P \approx 0.3\%$, in the temperature range 300-350 K (Lowndes and Martin, 1970), or, $\frac{1}{2}\left(\frac{\partial(\varepsilon_{stat}/\varepsilon_\infty)}{\partial\left(\frac{1}{kT}\right)}\right)_P \approx 10^{-8} eV$) are used in Eq. (7) and (5) to provide the EDL activation energy $E^{act} = 0.65(5)eV$ Accordingly, for the high temperature region (above 345 K), we obtain: $E^{act} = 0.01(1)eV$.

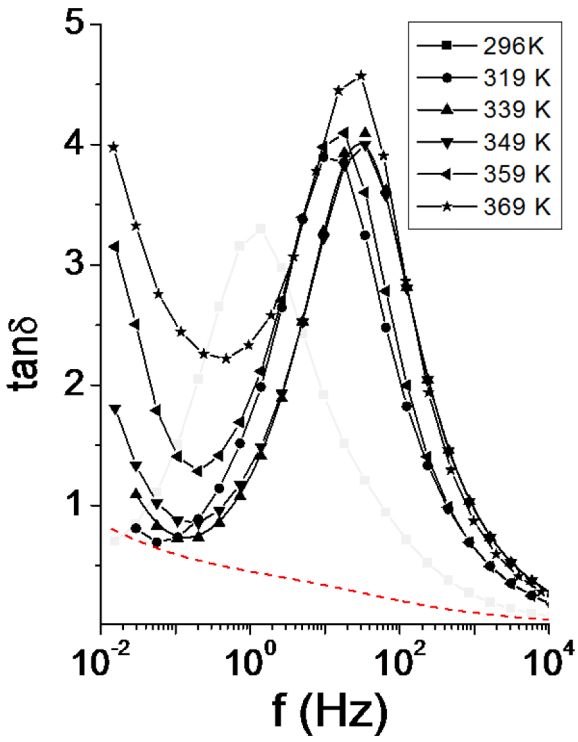

Fig. 1. Isotherms of the tangent loss angle of hydrated leukolite recorded at 270 MPa. Dash line is a reference measurement on a dry sample at 297 K.

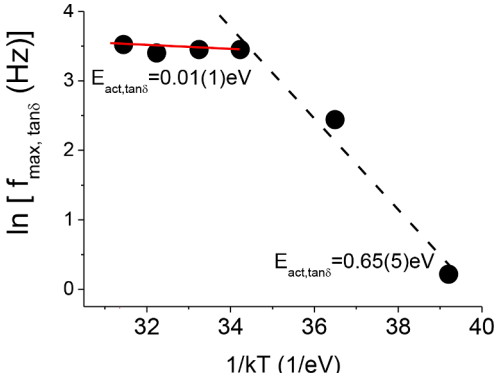

Fig. 2. The natural logarithm of the peak maximum $f_{max,\ tan\delta}$ as a function of reciprocal temperature at: 270 MPa. In the high temperature region, the maximum has a weak temperature dependence, evidencing for a nearly zero apparent activation energy of relaxation (an explanation is given in the text). In the low temperature region, the apparent activation energy is comparable the activation energy for charge transfer in dry leukolite, determined by high resolution Thermally Stimulated Relaxation Spectroscopy. Counter-ions in the Stern layer of water membrane are strongly coupled to electric charges in the solid phase.

5.2. Pressure dependence of the EDL relaxation

BDS experiments under hydrostatic pressure are valuable for identifying the nature of transferring charges and unravel different conduction mechanisms (Papathanassiou et al., 2000). It is hard to find theoretical and experimental works on how pressure affects the EDL relaxation. In Fig. 3, a sample of dielectric spectra at various pressures and constant temperature are depicted. We observe that, a tangent loss peak on increasing pressure, underlying the dc conductivity baseline at

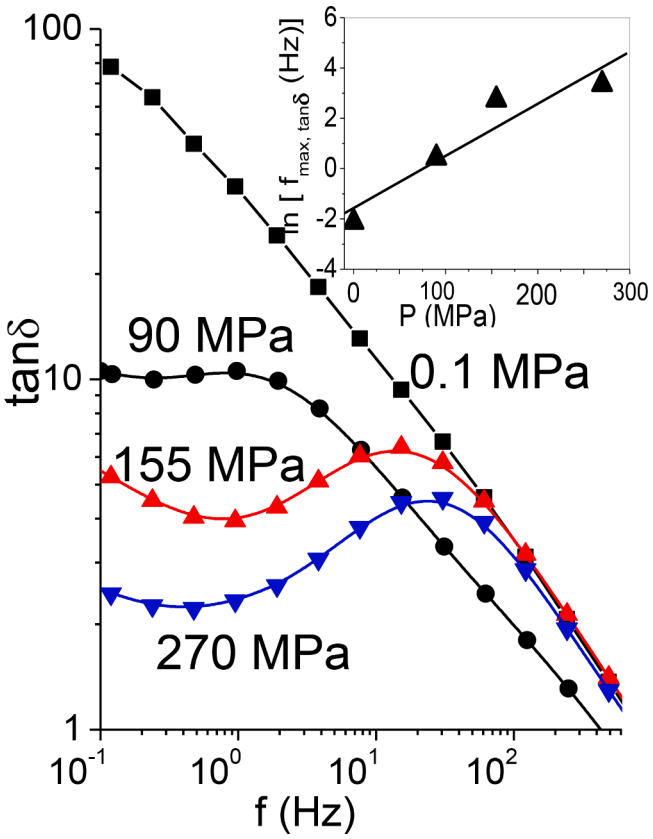

Fig. 3. Tangent loss angle spectra recorded at 370 K and different pressure values. Inset: the natural logarithm of the maximum (resonance) frequency as a function of pressure; the straight line that fits the data points, As explained in the text, its positive slope yields a negative activation volume for relaxation.

ambient pressure could, shifts towards high frequencies. A straight line fitted to the $lnf\,max, tan\delta$ (P) data points (inset diagram of Fig. 3), with slope: $\left(\frac{\partial lnf_{max,tan\delta}}{\partial P}\right)_T = +66(9)GPa^{-1}$.

Combined with $\left(\frac{\partial(\varepsilon_{stat}/\varepsilon_\infty)}{\partial P}\right)_T \approx -4.0(0)\ GPa^{-1}$ (Papathanassiou et al., 2010), Eq. (8) yields: $\left(\frac{\partial lnf_o}{\partial P}\right)_T = +64(8)C$. Eq. (6), thus, provides the value of the apparent activation volume $v^{app} = -1.3(3) \times 10^{-28} m^3$. The negative sign indicates that dielectric relaxation time becomes shorter upon compression, the main reason of which – according to Eq. (2) - is the enhancement of $D_s(P)$. One scenario for the negative sign of the activation volume is that, as mass of proton is small and quantum phenomena play a significant role to protonic conduction: by compressing the water molecules' network that wets a grain, the hopping range gets suppresses and proton exchange between neighboring water molecules in the Stern layer becomes easier to occur. Therefore, upon compression, the relaxation time for a two stage protonic transfer becomes, the relaxation frequency augments and $f_{max,tan\delta}$ increases and, hence, the negative activation volume. An alternative scenario for the negative sign, was suggested for protonic conductivity in NAFION membranes by by Fontanella and coworkers (Fontanella et al., 1996; Proton motion is usually interpreted as a transfer from a hydronium ion, H_3O^+, to a water molecule (Conway, 1964). The activation volume for ion motion is the volume change when a diffusing species transfers from a ground position to an activated position. A pair of a hydronium ion and a water molecule constitutes the ground state. The activated state consists of the co-existence of two water molecules sharing a proton. Because of the sharing, the activated state has, in principle, a smaller volume than the ground state, hence the activation volume for this process is negative.

The values of $v^{app}(T)$ are, within the experimental accuracy, insensitive to temperature (Fig. 4). While the $E_{app}(T)$ is characterized by a transition temperature around 345 K, $v^{app}(T)$ retains a constant value, indicating that the *nature* of the charge transfer is protonic, i.e., surface diffusion and conductivity, charge release from the EDL and charge exchange between the grain and the water membrane are dominated by proton transport.

6. Discussion

6.1. Effect of temperature

The temperature dependence of the relaxation time (in the temperature region explored in the present work) has two main sources:

(i) the thermally activated diffusivity, which can be described by an Arrhenius relation:$D_s = D_o exp$), where D_o is, as stated above, a constant pre-exponential factor and g is the Gibbs free energy for surface diffusion.

(ii) the temperature dependence of the charge carrier density parameter c, which is tuned by the competition between the thermal energy and absorption energy of layers wetting the solid grains. If the solid surface is considered as a two dimensional lattice (such as a Bragg-Williams lattice), the sites, which can be occupied (or, remain vacant), the energy balance of the interaction energy between absorbed charges and the liquid-solid interaction vs temperature, predicts a critical temperature T_c, above which, relaxing charges escape from the tight-birded Stern layer toward loose diffusion layers.

Differentiating Eq. (4) with respect to reciprocal temperature, we get::

$$-\left(\frac{\partial lnf_o}{\partial\left(\frac{1}{kT}\right)}\right)_P = -\left(\frac{\partial lnD_s}{\partial\left(\frac{1}{kT}\right)}\right)_P - \left(\frac{\partial ln(1+x)}{\partial\left(\frac{1}{kT}\right)}\right)_P \quad (9)$$

For a thermally activated surface diffusion, the diffusion coefficient is: $D_s = D_{so} exp\left(\frac{-g}{kT}\right)$, where D_{so} is constant (the temperature variation in the present study ensures a negligible change in the phonon frequencies involved in the flow event and, thus, D_{so} retains its constant value) and g denotes he Gibbs free energy for surface diffusion, i.e., $g = -\left(\frac{\partial lnD_s}{-\partial\left(\frac{1}{kT}\right)}\right)_P$.

The estimation of the last term of Eq. (9), i.e., requires a knowledge of $c(T)$. On increasing temperature, the thermal energy competes with the interaction energy w between water molecules banded on the solid

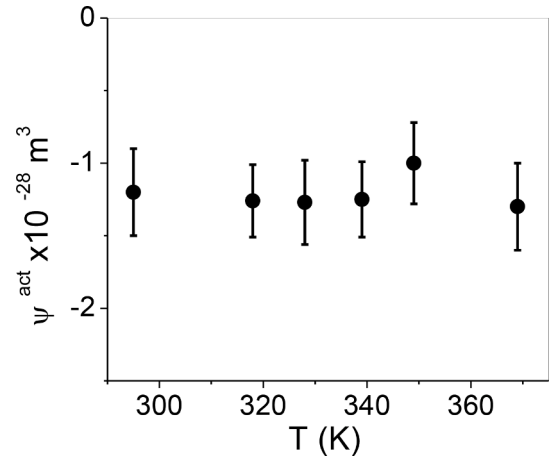

Fig. 4. Temperature dependence of the activation volume for dielectric relaxation.

surface. Consequently, the parameter c, which captures the number density of charges participating to the relaxation process at the membrane in direct contact with the solid, will reduce upon temperature. If we assume that the density charges reduce on heating according to:

$$c(T) = c_o e^{w/kT} \tag{10}$$

The variation of on reciprocal temperature is obtained through:

$$\left(\frac{\partial ln(1+x)}{\partial\left(\frac{1}{kT}\right)}\right)_P = \frac{1}{(1+x)}\left(\frac{\partial x}{\partial\left(\frac{1}{kT}\right)}\right)_P = w\frac{x}{1+x} \tag{11}$$

The term appearing in Eq. (3) is always positive, which implies that:. So, from Eq. (11), we get:

$$\left(\frac{\partial ln(1+x)}{\partial\left(\frac{1}{kT}\right)}\right)_P > 0 \tag{12}$$

We recall that Eq. (9) interconnects the *apparent* activation energy (estimated from the temperature evolution of the relaxation frequency), the Gibbs free energy for surface conduction and $x(T), as$:

$$E^{app} = g - \left(\frac{\partial ln(1+x)}{\partial\left(\frac{1}{kT}\right)}\right)_P \tag{13}$$

A positive value of the quantity $\left(\frac{\partial ln(1+x)}{\partial\left(\frac{1}{kT}\right)}\right)_P$ (according to Eq. (12)) implies that E^{act} *can possibly be found near - zero* (i.e., the relaxation time τ and its inverse relaxation rate$f_0 \equiv 1/\tau$, remain near - insensitive to of temperature changes). Our finding is in agreement with the prediction of observed zero – activation energy in a bi-phase system relaxing in NMR experiments (Korb et al., 2003).

- *Coupling of protonic conduction in the Stern potential with counter-ion transport within the grain, below 345 K*

Water molecules being in direct contact with a solid surface form a layer of reduced molecular translation and orientation mobility. However, water molecules are organized in a network of increased conduction. Grotthuss proposed a mechanism for proton transport between water molecules that involves the exchange of a covalent bond between H and O with a hydrogen bond (Grotthuss mechanisms (Miyake and Rolandi, 2016). Bond exchange is coupled with a reordering of the water network by the transport of an orientation defect (known as Bjerrum defect). The enhanced protonic conductivity results from the synergy between bond exchange and Bjerrum defect motion. The combined two stage process is thermally activated with an activation energy compared with the energy required to break a hydrogen bond, which is $0.1eV$ (Villegas-Jiménez et al., 2009). The latter is quite close to $E^{act} = 0.01(1)eV$ estimated for the high temperature region, rather than that determined for the low temperature region ($E^{act} = 0.65(5)eV$. However, the pressure experiments (Section 5.2) proved that, *in the entire temperature range* explored in this work, a unique protonic conduction of the relaxing species occurs. The corresponding activation volume values are, within the experimental accuracy, insensitive to temperature (Fig. 3).

To explain why, despite the fact that relaxation in the low temperature region involves protonic transport, a large energy for activation ($E^{act} = 0.65(5)eV$ is required, we recall earlier studies on *dry* leukolite: Thermally Stimulated Depolarization Current (TSDC) spectroscopy on as-received leukolite have been reported earlier (Papathanassiou, 1999). Experiments were carried out while the specimen was kept in continuous pumping by operating a turbo-molecular vacuum pump, in order to ensured the extraction of any traces of humidity that might naturally exist in the pores. A bulk conduction mechanism was detected and, employing various experimental TSDC schemes, attributed to a thermally activated charge transport (probably extrinsic cation impurities or vacancies) within the grains. The analyses of the spectra yielded a Gaussian distribution of the activation energy values around $E_o^{grain} = 0.72eV$and width parameter $\sigma_{Gauss} = 0.02eV$. This value is comparable to: $E^{act} = 0.65(5)eV$ found above below 345 K for the dielectric relaxation in hydrated leukolite, i.e.:: $E^{act} = 0.65(5)eV$. It is likely that, due to the strong coupling between processes in the grain and the water membrane, protonic conduction in the Stern layer is dominated by the counter-iom transport in the grain and, hence, the large activation energy for relaxation (based on protonic transfer), in the low temperature region.

- *The transition to a nearly zero activation energy for relaxation above 345 K*

Alkaline earth carbonate salts are regarded as practically insoluble in water. However, research on the interaction of calcium carbonate with aqueous solutions of various levels of acidity (pH ranged from nearly 7.0 to 9.5) indicated that fast proton/calcium exchange equilibrium between the solution and cation lattice at and/or beneath the calcite: $2CaCO_3 + 2H^+ \leftrightarrow 2Ca(HCO_3 + Ca^{2+}$, that leads tom α calcium-deficient, proton-enriched layer within the calcite lattice. Net proton sorption density estimated from acidimetric titrations, at $pH \rightarrow 7$, is around $2.6 \times 10^{-4} moles/m^2$ (Villegas-Jiménez et al., 2009).

Magnesite is an alkaline earth carbonate salt, thus, it is reasonable to assume that a magnesium cation/proton exchange occurs in wetted leukolite. In the present work, doubly distilled and doubly de-ionized water was introduced inside the pores of leukolite, thus, circumneutral conditions are established to the water membrane and a portion of surface and sub-surface cation lattice sites of the $MgCO_3$ grains are replaced by protons and the water membrane is enriched in Mg^{2+}. The ion exchange holds even if naturally occurring free ions are cited on the interior surface of the porosity of leukolite. In any case, the surface lattice sites and/or the sub-surface ones of magnesite grains are enriched in protons. The formation of either layers are shielding the protonic conduction along the water network organized on the grain surface from charges migrating in the bulk of magnesite grains. The phenomenon is amplified on increasing temperature, disturbs the coupling between surface protonic conduction along the water layer and migrating charges within the solid grain. Above about 345 K, decoupling is complete and protonic diffusion is not impeded by the migration of bulk transport in the solid. Hence, the activation energy for relaxation (which is controlled by the surface protonic mobility) changes its value from $E^{act} = 0.65(5)eV$ (comparable with E^{grain}=*0.72 eV*) at low temperatures to $E^{act} = 0.01(1)eV$ (close to the value $0.1eV$ (Wraight, 2006) of hydronium transfer in water) above the crossover temperature 345 K.,

6.2. *Effect of pressure*

Differentiating Eq. (4) with respect to pressure, we get:

$$-\left(\frac{\partial lnf_o}{\partial P}\right)_T = -\left(\frac{\partial lnD_s}{\partial P}\right)_T - \left(\frac{\partial ln(1+x)}{\partial P}\right)_T \tag{14}$$

We focus on the ratio $x \equiv \frac{4\pi\alpha}{\varepsilon_o(2\varepsilon_1+\varepsilon_2)}\frac{\epsilon e^2}{kT}$.: The role of the isothermal compressibility of the solid phase and the pressure dependence of the polarizabilities should be investigated for the solid-water system. The latter will be checked in the analysis of our experimental data. Generally, such dependencies are negligible compared with the experimental errors. Inspired from the theory of phase transitions, pressure suppresses the rate of desorption of water molecules from the tight bonded Stern layer.

In general, one can consider that pressure has the opposite effect of temperature on c, therefore: $\left(\frac{\partial c}{\partial P}\right)_T < 0$. Since $\left(\frac{\partial \alpha}{\partial P}\right)_T < 0$ and $\left(\frac{\partial \varepsilon}{\partial P}\right)_T > 0$ for

water (Floriano and Nascimento, 2004), we conclude that:,$\frac{\partial}{\partial P} ln(1+x) < 0$.

Combining Eq. (5) and (14), recalling that the activation volume for surface diffusion is:, we get:

$$\upsilon \cong kT\left\{ -\left(\frac{\partial lnf_o}{\partial P}\right)_T + \left(\frac{\partial ln(1+x)}{\partial P}\right)_T \right\}, \quad (15)$$

We observe that, which is obtained in BDS experiments, is reduced by the term, which is negatively signed, to provide the value of the activation volume υ.

- *Why $\upsilon^{app}(T)$ is constant, while $E^{app}(T)$ exhibits two different regions?*

Eq. (10) introduces the interaction between the Stern layer and its environment as a thermally activated reduction of the concentration c of the relaxing charge species. This aspect was experimentally justified for wetted carbonate salts (Section 6.1) as protons abandon the highly conducting water network developed on the solid surface by occupying cation lattice sites of the grain: i.e., these protons transduce from a state of high mobility to a localized state dictated by the strong interaction among lattice sites. Due to the cation/proton exchange, Mg^{2+}, the size of which is much larger than a single proton, The size mismatch and the reduced mobility of the cations makes them unfavorable to assist the enhanced protonic conductivity in the Stern layer and move toward the so-called diffusion region of water layers overlying the Stern one. The net process is described effectively by Eq. (10). Accordingly the surface and/or sub-surface proton-rich layer of the grain (which intermittent the protonic *bulk* conduction coupling, is built up gradually, on increasing temperature. The result of the thermally activated co-operation of the aforementioned processes is is the transition from a low temperature region to a high temperature one, where decoupling is dominating.

Pressure is expected to have a negligible effect on the charge release from the Stern layer: the water layer can easily rearrange themselves to reduce the configuration entropy abandon the Stern layer. Thus, υ^{app} captures volume fluctuation per each migrating (relaxing) charge entity. The volume change when a moving hydronium occupies its activated state in relation to its ground one, respectively, is independent on their concentration. On increasing temperature, this fluctuation volume (per hydronium) is unaffected by the (temperature induced) change in the concentration, hence, $\upsilon^{app}(T)$ is constant.

7. Conclusions

In the present work, the physics of the water – matrix EDL relaxation at elevated pressure and temperature is explored. Broadband Dielectric Spectroscopy at combined temperature and pressure conditions was conducted on natural polycrystalline magnesite (leukolite) wetted by water in its pore space. . The resulting activation volume indicates that protonic transport underlies the relaxation and it is practically constant upon temperature. The temperature evolution of the relaxation reveals two successive temperature regions: In the low temperature one, protonic surface transport couples to the conduction of point defects within the solid matrix. The slow charge transport in the solid embeds the motion of protons over the Stern water network. Above a critical temperature, a near – zero activation energy is observed. The phenomenon is attributed to the onset of a thermally activated fast protons - lattice cation exchange: a sub-surface solid layer enriched in lattice protons, while, released magnesium cations – due to size mismatch to the Stern water network - abandon the EDL toward overlying water layers. Our findings can simulate the physical properties of fluid containing rocks in the Earth's interior and probably contribute to the explanation of seismic electric signals.

Declaration of Competing Interest

The authors declare that they have no known competing financial interests or personal relationships that could have appeared to influence the work reported in this paper.

The authors declare the following financial interests/personal relationships which may be considered as potential competing interests:

Acknowledgments

We thank one of the reviewers for providing additional suitable reference.

References

Chelidze, T.L., Gueguen, Y., Ruffet, C., 1999. Electrical spectroscopy of porous rocks: a review II. Experimental results and interpretation. Geophys. J. Int. 137, 4. https://doi.org/10.1046/j.1365-246x.1999.00800.x, 16–3.

Conway, B. E., Modern Aspects of Electrochemistry No. 3; Bockris, J. O'M., Conway, B. E., Eds.; Butterworths: Washington, DC (1964) p 117.

Dukhin, S.S., Sorokina, T.V., Chelidze, T.L., 1969. On the theory of low-frequency polarization of coarse-grained disperse system. Kolloid Zhurnal 31, 823–830.

Endres, A.L., Knight, R.J., 1991. The effects of pore scale fluid distribution on the physical properties of partially saturated tight sandstone. Appl. Phys. 69, 1091–1098.

Floriano, W.B., Nascimento, M.A.C., 2004. Dielectric constant and density of water as a function of pressure at constant temperature. Braz. J. Phys. 38–41. https://doi.org/10.1590/S0103973320040001000006. Available from: <>Epub 27 Apr 2004. ISSN 1678-4448.

Fontanella, J.J., Edmondson, C.A., Wintersgill, M.C., Wu, Y., Greenbaum, S.G., 1996. High-pressure electrical conductivity and NMR studies in variable equivalent weight NAFION membranes. Macromolecules 29, 4944–4951. https://doi.org/10.1021/ma9600926.

Gast, R.G., East, P.J., 1964. Clays Clay Miner. 12, 297.

Korb, J.P, Godefroy, S, Fleury, M., 2003. Surface nuclear magnetic relaxation and dynamics of water and oil in granular packings and rocks. Magn. Reson. Imaging 3-4, 193–199. https://doi.org/10.1016/s0730-725x(03)00124-3. PMID: 12850707.

Korb, J.P., 2018. Multiscale nuclear magnetic relaxation dispersion of complex liquids in bulk and confinement. Prog. Nucl. Magn. Reson. Spectrosc. 104, 12–55. https://doi.org/10.1016/j.pnmrs.2017.11.001. Epub 2017 Nov 10. PMID: 29405980.

Lowndes, R.P., Martin, D.H., 1970. Dielectric constants of ionic crystals and their variations with temperature and pressure. Proc. R. Soc. Lond. A316, 351–375. https://doi.org/10.1098/rspa.1970.0084.

Miyake, T., Rolandi, Marco, 2016. From proton transport in proton wires to bioprotonic devices. J. Phys. 28, 023001.

Nettelblad, B., 1996. Electrical and dielectric properties of systems of porous solids and salt-containing nonpolar liquids. J. Appl. Phys. 79, 7106–7113. https://doi.org/10.1063/1.361480.

Papathanassiou, A.N., Sakellis, I., Grammatikakis, J., 2000. Separation of electric charge flow mechanisms in conducting polymer networks under hydrostatic pressure. Appl. Phys. Lett. 89, 222905 https://doi.org/10.1063/1.2768623.

Papathanassiou, A.N., Sakellis, I., Grammatikakis, J., 2007. Migration volume for polaron dielectric relaxation in disordered materials. Appl. Phys. Lett. 91, 202103 https://doi.org/10.1063/1.2812538.

Papathanassiou, A.N., Sakellis, I., Grammatikakis, J., 2010. Negative activation volume for dielectric relaxation in hydrated rocks. Tectonophysics 490, 307–309.

Papathanassiou, A.N., Sakellis, I., Grammatikakis, J., 2011. Dielectric property of Granodiorite partially saturated with water and its correlation to the detection of seismic electric signals. Tectonophysics 512, 148.

Papathanassiou, A.N., 1999. Thermal depolarisation studies in leukolite (polycrystalline magnesite ($MgCO_3$). J. Phys. Chem. Solids 60, 407–414. https://doi.org/10.1016/S0022-3697(98)00270-4.

Papathanassiou, A.N., 2000. Investigation of the dielectric relaxation and the transport properties of porous silicates containing humidity. Phys. Cond. Matter 12, 5789–5800. https://doi.org/10.1088/0953-8984/12/26/324.

Revil, A., Glover, P.W.J., 1997. Theory of ionic-surface electrical conduction in porous media. Phys. Rev. B 55, 1757.

Revil, A., 1999. Ionic diffusivity, electrical conductivity, membrane and thermoelectricpotentials in colloids and granular porous media: a unified model. J. Colloid Interface Sci. 212, 503–522.

Sakellis, I., Papathanassiou, A.N., Grammatikakis, 2014. Measurements of the dielectric properties of limestone under pressure and their importance for seismic electric signals. J. Appl. Geophys. 102, 77–80. https://doi.org/10.1016/j.jappgeo.2013.12.013.

Saltas, F.V., Gidarakos, E., 2013. Charge transport in diatomaceous earth studied by broadband dielectric spectroscopy. Appl. Clay Sci. 80-81, 226–235.

Saltas, V, Vallianatos, F., Triantis, D., 2008. Dielectric properties of non-swelling bentonite: the effect of temperature and water saturation. J. Non-Cryst. Solids 354 (52-54), 5533–5541.

Saltas, V., Chatzistamou, V., Pentari, D., Paris, E., Triantis, D., Fitilis, I., Valianatos, F., 2013. Complex electrical conductivity measurements of a KTB amphibolite sample at elevated temperatures. Mater. Chem. Phys. 139 (1), 169–175.

Saltas, V., Fitilis, I., Vallianatos, F., 2014. A combined complex electrical impedance and acoustic emission study in limestone samples under uniaxial loading. Tectonophysics 637, 198–206.

Sekine, T., 1986. Theory of dielectric relaxations due to the interfacial polarization for two-component suspensions of spheres. Colloid Polym. Sci. 264, 888–895. https://doi.org/10.1007/BF01410640.

Tzanis, A, Vallianatos, F., 2001. A critical review of ULF electric earthquake precursors. Ann. Geofisica 44/2, 429–460.

Vallianatos, F., Triantis, D., 2008. Scaling in pressure stimulated currents related with rock fracture. Physica A 387, 4940–4946.

Vallianatos, F., Triantis, D., Tzanis, A., Anastasiadis, C., Stavrakas, I., 2004. Electric earthquake precursors: from laboratory results to field observations. Phys. Chem. Earth 29, 339–351.

Varotsos, P., Alexopoulos, K., 1984. Physical properties of the variation of the electric field of the earth preceding earthquakes: determination of the epicenter and magnitude. Tectonophysics 110, 99–125.

Villegas-Jiménez, A, Mucci, A, Paquette, J., 2009. Proton/calcium ion exchange behavior of calcite. Phys. Chem. Chem. Phys. 39, 8895–8912. https://doi.org/10.1039/b815198a. Epub 2009 Jul 30. PMID: 20449036.

Wagner, K.W., 1924. Erklarung der Dielectrishen Nachwirkungsvorgange e3—dielectric permittivity of shell auf grund Maxwellscher vorstellungen. Arch. Electrotech. 2, 371–387 g—dynamic viscosity.

Wraight, C.A., 2006. Chance and design–proton transfer in water, channels and bioenergetic proteins. Biochim. Biophys. Acta 1757, 886–912.